Journal of Materials Chemistry

Cite this: J. Mater. Chem., 2012, 22, 2863

www.rsc.org/materials

COMMUNICATION

Self-powered high performance photodetectors based on CdSe nanobelt/graphene Schottky junctions

Weifeng Jin,[a] Yu Ye,[a] Lin Gan,[b] Bin Yu,[a] Peicai Wu,[a] Yu Dai,[a] Hu Meng,[a] Xuefeng Guo[b] and Lun Dai*[a]

Received 16th November 2011, Accepted 4th January 2012
DOI: 10.1039/c2jm15913a

Self-powered photodetectors based on CdSe nanobelt (NB)/graphene Schottky junctions are fabricated and investigated. Typically such Schottky junctions exhibit good rectifying behavior without light illumination. The on/off ratio is more than 1×10^5 when the voltage changes from −1 to 1 V. Under zero bias, typically such photodetectors show high photosensitivity ($\sim 3.5 \times 10^5$), which is defined as $(I_{photo} - I_{dark})/I_{dark}$, to above-band-gap irradiation. Under 1000 Hz light switching frequency, the response and recovery times of such photodetector are typically 82 and 179 μs, respectively, and the photoconductive gain is 28, greater than unity. The high photosensitivity and gain, as well as fast response speed, guarantee the feasibility of such self-powered photodetectors.

Introduction

Semiconductor-based photodetectors are one kind of optoelectronic device that can convert an optical signal into an electrical signal. The physical mechanism of photodetection is the generation of electron–hole (e–h) pairs through optical absorption of incident photons. The photogenerated e–h pairs are then separated and collected to the external circuit by an electric field. Generally, the electric field can be supplied by either a build-in electric field in a junction (such as p–n,[1] p–i–n,[2,3] or Schottky junction[4,5] photodetectors), or an external power supply (such as photoconductor-based photodetectors[6,7]). Basically, the former can work without an external power supply, which is highly desired with regards to the global energy crisis.

Compared to traditional photodetectors based on bulk or thin film materials, nanowire/nanobelt (NW/NB) photodetectors have unique characteristics because of the large surface-to-volume ratio and reduced dimensionality. Soci *et al.*[8] demonstrated that the high-density surface trap states on NWs had a significant influence on their photoresponse and gain. Compared to a p–n junction, a Schottky junction has the advantage of material universality, facile fabrication processes *etc.* However, the remarkable light absorption of metals will seriously limit the performance of the photodetectors made from a Schottky junction. Yang *et al.*[4] have reported a kind of self-powered ultraviolet detector based on a ZnO NB/Au Schottky junction. However, the photosensitivity is only 22 with a slow photoresponse speed (~100 ms). Little work on self-powered visible-light photodetectors based on NWs or NBs with high performance has been reported so far.

Graphene has some fascinating properties, such as high carrier conductivity and optical transparency, which predict its huge potential application in novel optoelectronic devices.[9,10] So far, graphene has been used to substitute indium titanium oxide (ITO) as the flexible transparent conductive electrode for organic photovoltaics[11] and light-emitting diodes (LEDs),[12] since ITO has the drawbacks of high-cost, limited use for flexible substrates, and degradation of device performance over time due to indium diffusion. In this paper, we use graphene as a substitute for metal and fabricate self-powered CdSe NB/graphene Schottky junction photodetectors. Owing to the work function difference between CdSe (4.2 eV)[13] and graphene (4.6 eV),[14,15] a Schottky junction can form between graphene and the CdSe NBs. Under zero bias, such photodetector typically shows a high photosensitivity (~3.5×10^5) to above-band-gap irradiation (>1.75 eV[16] at room temperature) and a fast response (with response and recovery times of 82 μs and 179 μs, respectively) in a wide range of switching frequencies (up to 1000 Hz). The photoconductive gain is 28, greater than unity.

Experiments

The n-type CdSe NBs and monolayer graphene used in this work were synthesized *via* chemical vapor deposition (CVD).[17] For synthesis of CdSe NBs, CdSe powder (99.995%), placed in the upstream of Ar gas current, was used as the source. Pieces of Si wafers covered with 10 nm thick thermally evaporated Au films were used as substrates. A tiny Cd grain (99.95%) was placed between the source and the substrates as the dopant. The temperatures at the source and substrates were about 870 °C and 650–750 °C, respectively. The as-synthesized CdSe NBs exhibited n-type conductivity due to selenium vacancies or cadmium interstitial atoms, which serve as shallow donors in CdSe.

For the synthesis of large-scale uniform monolayer graphene,[18] a quartz boat loaded with Cu foil was placed in a tube furnace. Then the system was evacuated and heated to 1000 °C under a 10 cm^3 min^{-1} flow rate of H_2 at a pressure of about 50 Pa. After stabilizing the temperature at 1000 °C, CH_4 with a flow rate of 1.1 cm^3 min^{-1} was introduced at a pressure of about 60 Pa for 15 min. After the

[a]*State Key Lab for Mesoscopic Physics and School of Physics, Peking University, Beijing, 100871, China. E-mail: lundai@pku.edu.cn*
[b]*College of Chemistry and Molecular Engineering, Peking University, Beijing, 100871, China*

growth, the substrates were cooled down to room temperature. It should be noted that during the whole process, the flow rate of H_2 is kept constant at 10 cm^3 min^{-1}.

The transfer of synthesized graphene to the Si/SiO_2 substrate was carried out with the help of poly methyl methacrylate (PMMA).[19] First, a layer of PMMA (200 nm) was spun on the graphene. Then, the sample was immersed into 1 M $FeCl_3$ solution for ~3 h to etch off the underlying Cu foil. After that, the graphene/PMMA film was rinsed in deionized water to remove the residual metal ions.

The device fabrication processes were as follows: first the CdSe NBs were dispersed in ethanol with an ultrasonic process. Then, the CdSe NB suspension solution was dropped onto an oxidized Si substrate with a 600 nm SiO_2 layer on the top. After that, an In/Au (10/100 nm) ohmic contact electrode was defined on one end of a CdSe NB with photolithography followed by thermal evaporation and lift-off process. Later, the graphene/PMMA film floating on the deionized water was manually collected onto the device substrate. Heat treatment (75 °C under air for 10 min) was adopted to further strengthen the adhesion between the substrate and the graphene/PMMA film. After that, PMMA was removed by acetone. Finally, a graphene pad was defined at the other end of the CdSe NB using photolithography followed by inductive coupled plasma (ICP) etching. An Au (100 nm) electrode, which can form an ohmic contact with the graphene, was fabricated on the graphene away from the NB for welding purpose.

The photodetector was imaged using a field-emission scanning electron microscope (FESEM) (FEI NanoSEM 430). The photoluminescence (PL) and Raman spectra were collected on a microzone confocal Raman spectroscope (HORIBA Jobin Yvon, LabRam HR800). The transparency characterization was done using a UV-vis-NIR recording spectrophotometer (Shimadzu UV-3100). Room-temperature electrical transport properties of the CdSe NB/graphene Schottky photodetectors were measured with a semiconductor characterization system (Keithley 4200). The electrical properties of graphene were characterized by a Hall measurement system (Accent HL5500).

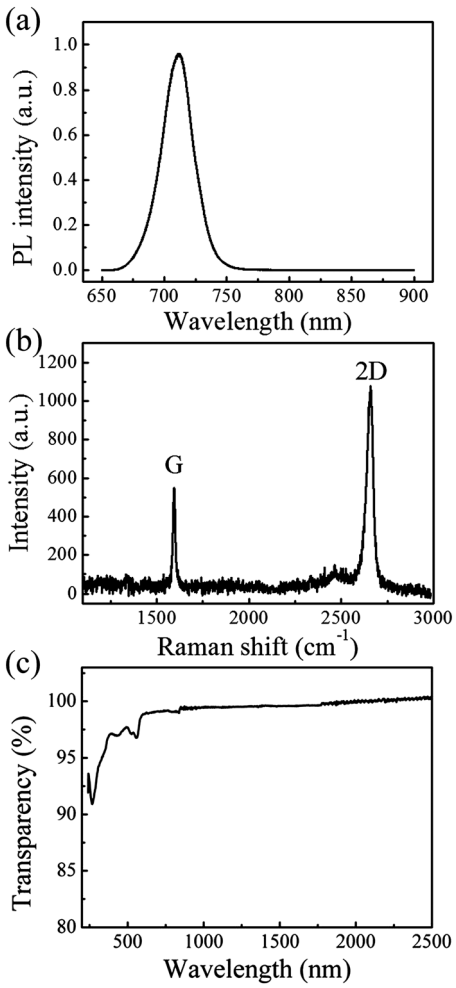

Fig. 1 (a) Typical room-temperature PL spectrum of a CdSe NB. (b) Typical Raman spectrum of the graphene on a Si/SiO_2 substrate. (c) The transparency spectrum of the graphene on a quartz substrate.

Results and discussion

Fig. 1a shows the typical room-temperature PL spectrum of the as-synthesized CdSe NBs. A strong near-bandgap emission at around 710 nm as well as no defect related emission reveals the high quality of the CdSe NBs. Fig. 1b shows the Raman spectrum of the graphene transferred onto a 600 nm Si/SiO_2 substrate. Two peaks at 1593 cm^{-1} (G peak) and 2658 cm^{-1} (2D peak) can be observed clearly. The ratio of G to 2D peak intensity is ~0.51, indicating the formation of monolayer graphene.[20] Furthermore, no defect related D peak (~1350 cm^{-1}) can be observed within the resolution of the Raman spectroscope, indicating the high quality of the graphene. Fig. 1c shows the transparency spectrum of the graphene. In order to do this measurement, the as-grown graphene was transferred to a quartz substrate. High transparency (>97%) can be seen in the wavelength range from 400 to 2500 nm. The sheet resistance, hole concentration, and hole mobility of the graphene, measured by the Hall measurement, are about 345 Ω sq^{-1}, 1.84 × 10^{14} cm^{-2}, and 98.6 cm^2 V^{-1} s^{-1}, respectively.

Fig. 2a shows an FESEM image of an as-fabricated CdSe NB/graphene Schottky junction photodetector. From this figure, we can see the uniform width of the CdSe NB as well as the intimate contact between graphene and the CdSe NB. Fig. 2b and c show the energy band diagrams of the self-powered photodetector connected in short circuit and with an external resistor, respectively. With Fig. 2b, c, we can explain the mechanism of the self-powered photodetector qualitatively as follows: because of the work function difference between the two materials, a built-in electric field forms between graphene and the CdSe NB. Upon above-band-gap light illumination, the photogenerated holes and electrons are driven towards the graphene and the CdSe NB, respectively, by the built-in field, resulting in a short-circuit current or a voltage drop on the external resistor. In Fig. 2c, the offset between the quasi-Fermi levels of the CdSe NB and graphene results from the voltage drop on the external resistor, which is analogous to applying a forward bias to the Schottky junction.

The room-temperature I–V curve of the Schottky junction shows a rectification behavior as shown in Fig. 3a. The on/off current ratio is more than 1 × 10^5 when the voltage changes from −1 to 1 V. The turn-on voltage is around 0.6 V. For Schottky junctions made of semiconductors with high mobility, such as CdSe, the carrier transport mechanism can be modeled by thermionic emission theory.[21] Therefore, by fitting the measured I–V curve with the equation $I = I_0[\exp(eV/n\kappa T) - 1]$, where I_0 is the reverse saturation current, e is the electron charge, V is the applied bias, n is the diode ideality factor, κ is

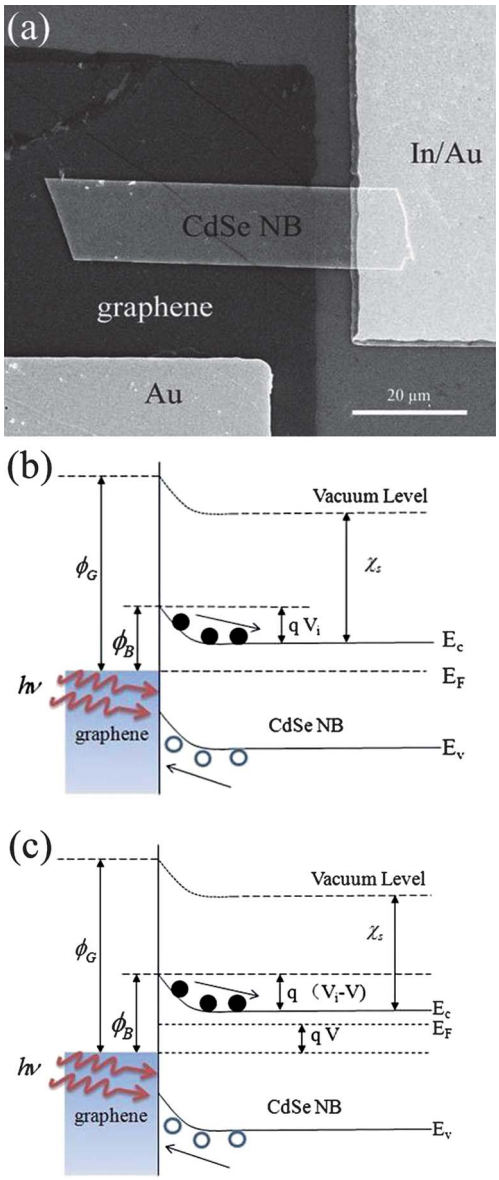

Fig. 2 (a) An FESEM image of the photodetector. (b) and (c) The energy band diagrams of such photodetector under light illumination for the short-circuited and load (resistor) cases, respectively. Φ_G is the work function of graphene, Φ_B is the Schottky barrier height, V_i is the built-in potential, V is the voltage drop on the resistor, χ_s is the electron affinity of the CdSe NB. E_C, E_V, and E_F are the conduction band edge, valence band edge, and Fermi level of the CdSe NB, respectively.

the Bolzmann constant, and T is the absolute temperature, we obtain $n = 1.52$.

The photocurrent response of a typical CdSe NB/graphene Schottky junction photodetector measured at zero bias voltage (under short circuit conditions) was investigated under fixed white light illumination. The typical result is shown in Fig. 3b. From this figure, we can see that the photosensitivity of the photodetector is about 3.5×10^5, among the best values reported so far for Schottky junction based photodetectors. We attribute the high photosensitivity to the high optical transparency and conductivity of the graphene, as well as the high quality of the CdSe NB with a large surface-to-volume ratio.

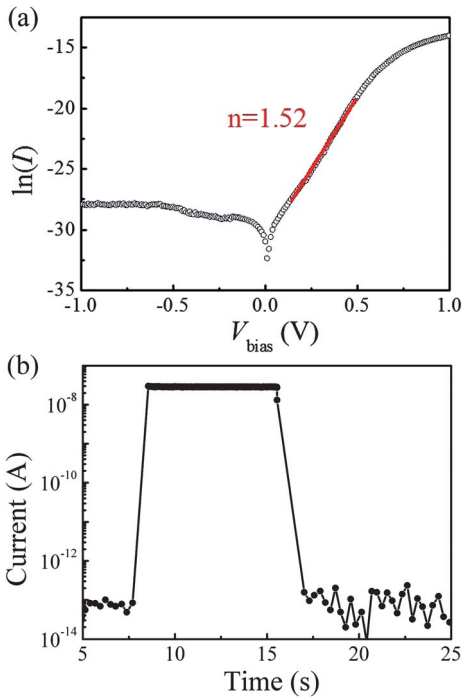

Fig. 3 (a) Current–voltage (I–V) characteristic of the device without illumination on a semi-log scale. The red straight line shows the fitting result of the I–V curve by the equation $\ln(I) = (eV/n\kappa T) + \ln(I_0)$. (b) Photocurrent response measured at zero bias (under short circuit conditions) under a fixed white light illumination.

Speed is another key parameter of a photodetector in light-wave communication and optical switch applications. In order to measure the speed of the photodetectors, we used a mechanical light chopper, a 633 nm He–Ne laser, and an oscilloscope (Tektronix DPO2024) to construct the experimental set-up, as shown in Fig. 4a. The resistor was 1 MΩ. Fig. 4b shows the photocurrent response of the self-powered photodetector under 1000 Hz light switching frequency, which was obtained by measuring the voltage drop on the resistor. Fig. 4c shows a single normalized modulation cycle measured at 1000 Hz, where the red and blue lines represent the rising and falling edges, respectively. The photoresponse time is defined as the time required for photocurrent to increase from 10% to 90% of I_{peak}, and the recovery time is defined analogously. Thus, we can obtain the response and the recovery times to be about 82 and 179 μs, respectively. It is worth noting that the response and recovery times could be further reduced by increasing the light power density.[22] Also, we can estimate the response (τ_{resp}) and recovery (τ_{rec}) time constant to be 12 μs and 132 μs, respectively, by fitting the rising and falling edges with equations $I = I_0[1 - \exp(-t/\tau_{resp})]$ and $I = I_0\exp(-t/\tau_{rec})$.

The current responsivity and photoconductive gain are two critical parameters that characterize photodetectors. The responsivity, R_λ, is defined as the photocurrent generated per unit power of the incident light on the effective area of a photodetector. The photoconductive gain, G, is defined as the number of electrons produced in the external circuit for each absorbed incident photon. The responsivity and gain[23] can be described as $R_\lambda = \Delta I/(P_{opt} \times S)$ and $G = [\Delta I/(P_{opt} \times S \times \eta)] \times (h\nu/e)$, respectively. Herein, ΔI is the difference between photocurrent and dark current, P_{opt} is the incident light power density (~2.7 mW cm^{-2}), S is the area of the Schottky junction

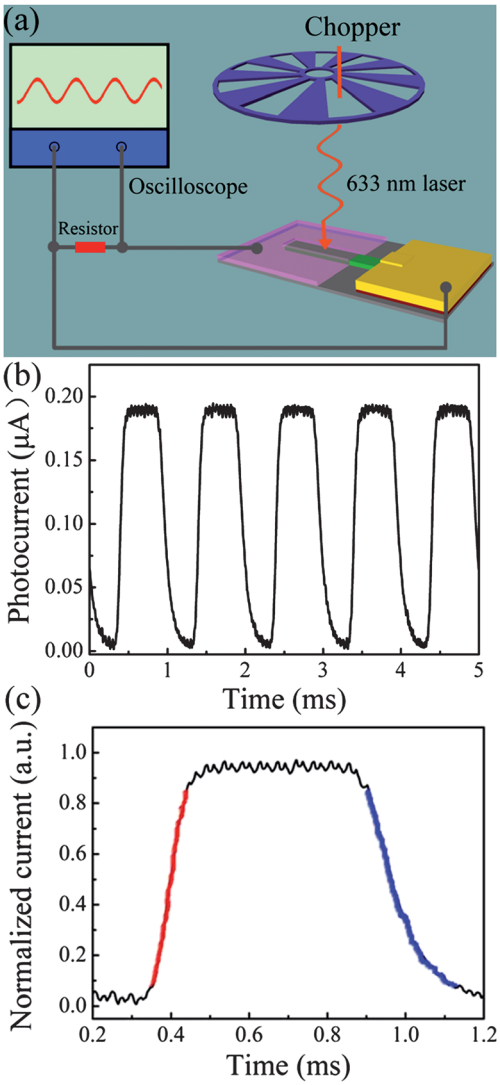

Fig. 4 (a) Schematic diagram of our experimental setup for photodetector speed measurement; (b) photocurrent response of the photodetector under a 1000 Hz light switching frequency; (c) a single normalized modulation cycle measured at 1000 Hz. The red and blue lines represent the rising and falling edges, respectively.

(~652.5 μm^2), e is the electron charge, h is Planck's constant, ν is the frequency of the 633 nm incident light (~4.7 × 10^{14} Hz), η is effective photocarrier generation efficiency (assumed to be 0.7 in this work, taking the reflection, scattering, and incomplete absorption *etc.* into consideration). According to Fig. 4b, we can estimate the responsivity to be about 10.2 A W^{-1} and gain to be about 28, greater than unity, under 1000 Hz switching frequency. The origin of greater-than-unity gain may be explained as follows: Se vacancies, which usually exist abundantly on the CdSe NB surface, would adsorb oxygen molecules from the ambient environment.[22] The adsorbed oxygen molecules may capture the free electrons, resulting in a depletion layer in the NB conductive channel. Upon above-band-gap light illumination, photogenerated holes may be driven to the surface of the NB by the built-in electric field in the depletion layer and discharge the negatively charged adsorbed oxygen ions and desorb oxygen from the NB surface.[8] Namely, oxygen adsorption and desorption on the CdSe NB surface plays a role in hole-trapping and prolongs the mean hole lifetime. If the hole mean lifetime is longer than the electron mean transit time, the gain can be greater than unity. The photogenerated holes may also be trapped in either depletion region of the Schottky junction or in surface states at the CdSe NB/graphene interface. It would shrink the width of Schottky barrier and permits more electrons to be injected into CdSe NB, leading to a greater-than-unity gain.[24] If we take the mechanical chopping process into consideration, the light switching process should take several microseconds. It means the real response and recovery times of the photodetectors should be even shorter. On the other hand, we think that the fast speed of photodetectors may benefit from the large surface-to-volume ratios of the CdSe NB and graphene, which may, in some way, help increase the carrier recombination rate. We attribute the high performance of the photodetectors to the short transit time and proper minority carrier mean lifetime.

Conclusion

In conclusion, we have fabricated and investigated high-performance self-powered photodetectors, which is based on the CdSe NB/graphene Schottky structure. The typical rectification ratio of such a Schottky junction is greater than 1 × 10^5. Under zero bias, such photodetectors typically show high photosensitivity and short response and recovery times. We attribute the high photosensitivity and gain as well as fast speed of the self-powered photodetectors to the high quality of graphene and CdSe NB used. This kind of high-performance photodetector, with the advantages of easy fabrication and energy-saving, shows huge application potential in the fields of visible-light detecting, binary switches, and optoelectronic integrated circuits.

Acknowledgements

This research was supported by the National Natural Science Foundation of China (No. 61125402, 51172004, 11074006), and the National Basic Research Program of China (No. 2012CB932703).

References

1 H. Zhu, C. X. Shan, B. Yao, B. H. Li, J. Y. Zhang, D. X. Zhao, D. Z. Shen and X. W. Fan, *J. Phys. Chem. C*, 2008, **112**, 20546–20548.
2 J. M. Zhang and D. R. Conn, *J. Lightwave Technol.*, 1992, **10**, 603–609.
3 F. Sun, C. X. Shan, S. P. Wang, B. H. Li, Z. Z. Zhang, C. L. Yang and D. Z. Shen, *Mater. Chem. Phys.*, 2011, **129**, 27–29.
4 Y. Yang, W. Guo, J. J. Qi, J. Zhao and Y. Zhang, *Appl. Phys. Lett.*, 2010, **97**, 223113.
5 S. Liang, H. Sheng, Y. Liu, Z. Huo, Y. Lu and H. Shen, *J. Cryst. Growth*, 2001, **225**, 110–113.
6 P. C. Wu, Y. Dai, Y. Ye, Y. Yin and L. Dai, *J. Mater. Chem.*, 2011, **21**, 2563–2567.
7 H. Kind, H. Q. Yan, B. Messer, M. Law and P. D. Yang, *Adv. Mater.*, 2002, **14**, 158–160.
8 C. Soci, A. Zhang, B. Xiang, S. A. Dayeh, D. P. R. Aplin, J. Park, X. Y. Bao, Y. H. Lo and D. Wang, *Nano Lett.*, 2007, **7**, 1003–1009.
9 A. K. Geim and K. S. Novoselov, *Nat. Mater.*, 2007, **6**, 183–191.
10 H. B. Heersche, P. J. Herrero, J. B. Oostinga, L. M. K. Vandersypen and A. F. Morpurgo, *Nature*, 2007, **446**, 56–59.
11 J. B. Wu, H. A. Becerril, Z. N. Bao, Z. F. Liu and Y. S. Chen, *Appl. Phys. Lett.*, 2008, **92**, 263302.
12 Y. Ye, L. Gan, L. Dai, H. Meng, F. Wei, Y. Dai, Z. J. Shi, B. Yu, X. F. Guo and G. G. Qing, *J. Mater. Chem.*, 2011, **21**, 11760–11763.
13 L. H. Zhang, Y. Jia, S. S. Wang, Z. Li, C. Y. Ji, J. Q. Wei, H. W. Zhu, K. L. Wang, D. H. Wu, E. Z. Shi, Y. Fang and A. Y. Cao, *Nano Lett.*, 2010, **10**, 3583–3589.

14 Y. M. Shi, K. K. Kim, A. Reina, M. Hofmann, L. J. Li and J. Kong, *ACS Nano*, 2010, **4**, 2689–2694.
15 Y. Ye, L. Gan, L. Dai, Y. Dai, X. F. Guo, H. Meng, B. Yu, Z. J. Shi, K. P. Shang and G. G. Qing, *Nanoscale*, 2011, **3**, 1477–1481.
16 S. Dayal, N. Kopidakis, D. C. Olson, D. S. Ginley and G. Rumbles, *Nano Lett.*, 2010, **10**, 239–242.
17 C. Liu, P. C. Wu, T. Sun, L. Dai, Y. Ye, R. M. Ma and G. G. Qin, *J. Phys. Chem. C*, 2009, **113**, 14478–14481.
18 L. Gan, S. Liu, D. N. Li, H. Gu, Y. Cao, Q. Shen, Z. X. Wang, Q. Wang and X. F. Guo, *Acta Phys. Chim. Sin.*, 2010, **26**, 1151–1156.
19 X. S. Li, Y. W. Zhu, W. W. Cai, M. Borysiak, B. Y. Han, D. Chen, R. Piner, L. Colombo and R. S. Ruoff, *Nano Lett.*, 2009, **9**, 4359–4363.
20 X. S. Li, W. W. Cai, J. H. An, S. Kim, J. Nah, D. X. Yang, R. Piner, A. Velamakanni, I. Jung, E. Tutuc, S. K. Banerjee, L. Colombo and R. S. Ruoff, *Science*, 2009, **324**, 1312–1314.
21 B. L. Sharma, *Metal-Semiconductor Schottky Barrier Junctions and Their Applications*, Plenum Press, New York, 1984.
22 Y. Jiang, W. J. Zhang, J. S. Jie, X. M. Meng, X. Fan and S. T. Lee, *Adv. Funct. Mater.*, 2007, **17**, 1795–1800.
23 S. C. Kung, W. D. Xing, W. E. Veer, F. Yang, K. C. Donavan, M. Cheng, J. C. Hemminger and R. M. Penner, *ACS Nano*, 2011, **5**, 7627–7639.
24 R. R. Mehta and B. S. Sharma, *J. Appl. Phys.*, 1973, **44**, 325–328.